




HIV DNA-Adenovirus Multiclade Envelope Vaccine Induces gp41 Antibody Immunodominance in Rhesus Macaques

 Qifeng Han,^a Wilton B. Williams,^a Kevin O. Saunders,^a Kelly E. Seaton,^a Kevin J. Wiehe,^a Nathan Vandergrift,^a Tarra A. Von Holle,^a Ashley M. Trama,^a Robert J. Parks,^a Kan Luo,^a Thaddeus C. Gurley,^a Thomas B. Kepler,^b Dawn J. Marshall,^a David C. Montefiori,^a Laura L. Sutherland,^a Munir S. Alam,^a John F. Whitesides,^a Cindy M. Bowman,^a Sallie R. Permar,^a Barney S. Graham,^c John R. Mascola,^c Patrick C. Seed,^d Koen K. A. Van Rompay,^e Georgia D. Tomaras,^a M. Anthony Moody,^a Barton F. Haynes^a

Duke Human Vaccine Institute, Duke University School of Medicine, Durham, North Carolina, USA^a; Department of Microbiology, Boston University, Boston, Massachusetts, USA^b; Vaccine Research Center, NIH, Bethesda, Maryland, USA^c; Department of Molecular Genetics and Microbiology, Duke University School of Medicine, Durham, North Carolina, USA^d; California National Primate Research Center, University of California, Davis, California, USA^e

ABSTRACT Dominant antibody responses in vaccinees who received the HIV-1 multiclade (A, B, and C) envelope (Env) DNA/recombinant adenovirus virus type 5 (rAd5) vaccine studied in HIV-1 Vaccine Trials Network (HVTN) efficacy trial 505 (HVTN 505) targeted Env gp41 and cross-reacted with microbial antigens. In this study, we asked if the DNA/rAd5 vaccine induced a similar antibody response in rhesus macaques (RMs), which are commonly used as an animal model for human HIV-1 infections and for testing candidate HIV-1 vaccines. We also asked if gp41 immunodominance could be avoided by immunization of neonatal RMs during the early stages of microbial colonization. We found that the DNA/rAd5 vaccine elicited a higher frequency of gp41-reactive memory B cells than gp120-memory B cells in adult and neonatal RMs. Analysis of the vaccine-induced Env-reactive B cell repertoire revealed that the majority of HIV-1 Env-reactive antibodies in both adult and neonatal RMs were targeted to gp41. Interestingly, a subset of gp41-reactive antibodies isolated from RMs cross-reacted with host antigens, including autologous intestinal microbiota. Thus, gp41-containing DNA/rAd5 vaccine induced dominant gp41-microbiota cross-reactive antibodies derived from blood memory B cells in RMs as observed in the HVTN 505 vaccine efficacy trial. These data demonstrated that RMs can be used to investigate gp41 immunodominance in candidate HIV-1 vaccines. Moreover, colonization of neonatal RMs occurred within the first week of life, and immunization of neonatal RMs during this time also induced a dominant gp41-reactive antibody response.

IMPORTANCE Our results are critical to current work in the HIV-1 vaccine field evaluating the phenomenon of gp41 immunodominance induced by HIV-1 Env gp140 in RMs and humans. Our data demonstrate that RMs are an appropriate animal model to study this phenomenon and to determine the immunogenicity in new HIV-1 Env trimer vaccine designs. The demonstration of gp41 immunodominance in memory B cells of both adult and neonatal RMs indicated that early vaccination could not overcome gp41 dominant responses.

KEYWORDS HIV-1 envelope, gp41, rhesus macaques, HIV-1 vaccine, microbiome

Received 12 June 2017 Accepted 31 July 2017

Accepted manuscript posted online 9 August 2017

Citation Han Q, Williams WB, Saunders KO, Seaton KE, Wiehe KJ, Vandergrift N, Van Holle TA, Trama AM, Parks RJ, Luo K, Gurley TC, Kepler TB, Marshall DJ, Montefiori DC, Sutherland LL, Alam MS, Whitesides JF, Bowman CM, Permar SR, Graham BS, Mascola JR, Seed PC, Van Rompay KKA, Tomaras GD, Moody MA, Haynes BF. 2017. HIV DNA-adenovirus multiclade envelope vaccine induces gp41 antibody immunodominance in rhesus macaques. *J Virol* 91:e00923-17. <https://doi.org/10.1128/JVI.00923-17>.

Editor Guido Silvestri, Emory University

Copyright © 2017 American Society for Microbiology. All Rights Reserved.

Address correspondence to Barton F. Haynes, barton.haynes@dm.duke.edu.

Recombinant monoclonal antibodies (MAbs) isolated from blood plasmablasts of individuals with acute HIV-1 infection predominantly targeted Env gp41 and were polyreactive with both host and environmental antigens, including members of the intestinal microbiota (1–3). Polyreactive gp41-binding MAbs can also be isolated from blood of uninfected individuals, suggesting that the HIV-1 Env gp41-reactive Abs induced during acute HIV-1 infection originated from a subset of gp41 cross-reactive memory B cells previously activated by non-HIV-1 antigens (2, 3). Similarly, in the terminal ileum in HIV-1 infected and uninfected individuals, mutated Env gp41-reactive MAbs were found to cross-react with members of the intestinal microbiota (3).

In the setting of vaccination, the multiclade (A, B, and C) DNA/recombinant adenovirus virus type 5 (rAd5) vaccine in phase 2a and 2b trials (4, 5) induced Env-reactive Ab responses that were dominated by gp41-reactive Abs (6). Vaccine-induced gp41-reactive Abs were nonneutralizing and cross-reacted with host antigens as well as with bacterial proteins RNA polymerase and pyruvate-flavodoxin oxidoreductase, which shared sequence similarities with the heptad repeat 1 region of HIV-1 gp41 (6). Interestingly, pre- and postvaccination clonally related Abs from DNA/rAd5-vaccinated individuals were reactive with both gp41 and members of the intestinal microbiota, but the postvaccination Ab was more affinity matured than the prevaccination Ab, suggesting that the vaccine-induced Ab response originated from a preexisting pool of gp41-microbiota cross-reactive B cells (6). In a second human clinical trial, HIV-1 Vaccine Trials Network (HVTN) trial 205, a DNA prime and MVA boost with gp140 also induced gp41-dominant plasma responses in humans, with titers of gp41-specific IgG higher than those of gp120-specific IgG (7). These studies indicated that two gp41-containing immunogens induced a dominant gp41-reactive Ab response in humans.

Rhesus macaques (RMs) are widely used to investigate human HIV-1 pathogenesis and have utility for testing preclinical efficacy of prevention strategies, including candidate vaccines (8–11). Thus, determining if gp41-containing immunogens in HIV-1 vaccines induce a dominant gp41 response in RMs is key to defining if RMs are an appropriate animal model for evaluation of Env-containing vaccines.

Studies have suggested that microbial antigens can stimulate immune cells and expand CD4⁺ T cells and B cell repertoires (12–19). For example, the intestines of germfree mice have low numbers of lamina propria CD4⁺ T cells compared to bacterially colonized mice (12). Microbial colonization also influences early B-lineage development and leads to increased receptor editing, suggesting that the gut microbes may shape the preimmune repertoire in gut lamina propria (16). Thus, a hypothesis is that vaccination early in bacterial imprinting of the B cell repertoire may shape the immune response to vaccine immunogens.

Here we demonstrate that the DNA/rAd5 vaccine induced a dominant gp41-reactive Ab response in RMs. Vaccine-induced gp41-reactive RM MAbs were cross-reactive with autologous intestinal microbiota, similar to gp41-microbiota cross-reactive human MAbs induced by DNA/rAd5 vaccine. Moreover, neonatal RMs immunized during the time of postnatal microbial colonization also manifested a gp41-dominant Ab response to the DNA/rAd5 vaccine.

RESULTS

Neonatal and adult RM vaccination with the DNA/rAd5 trivalent Env vaccine.

The plasma of both neonatal and adult RMs immunized with the DNA/rAd5 vaccine displayed similar reactivities with HIV-1 gp41 and gp120 recombinant proteins at 4 weeks after rAd5 boost (*P* value was not significant [NS]; Wilcoxon signed-rank test) (Fig. 1A, B, and C), the identical time point studied with this vaccine in humans (6). However, one adult RM showed lower titers of plasma Ab to gp120 than to gp41. Thus, the DNA/rAd5 vaccine induced similar plasma levels of HIV-1 Env gp41 and gp120-targeted Abs in RMs. We also compared the plasma neutralizing Ab responses elicited by DNA/rAd5 vaccine in neonatal and adult RMs and found that neonates responded as well as or better than adults to the DNA/rAd5 vaccine and in the TZM-bl assay neutralized more easy-to-neutralize (tier 1) virus isolates, such as SF162 and Bal.26, than

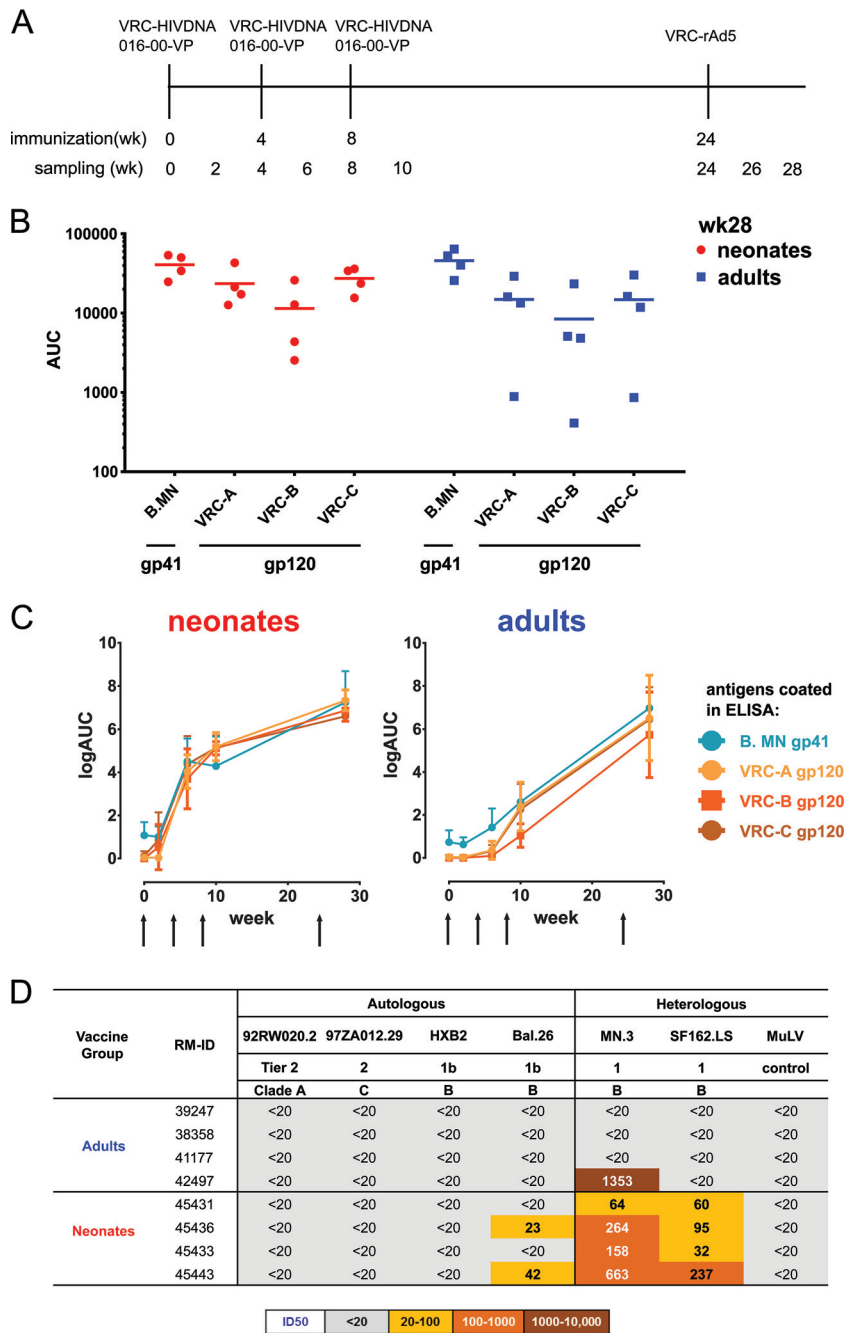


FIG 1 Plasma Ab binding and neutralization profiles of DNA/rAd5-vaccinated RMs. (A) DNA/rAd5 vaccinations in 4 neonatal RMs and 4 adult RMs. RMs were immunized with DNA prime 3 times, with an rAd5 boost. PBMCs and plasma were collected on the vaccination day and at 2 weeks after each vaccination, with sampling time points indicated on the vaccination timeline; vaccine-induced Ab repertoires of blood memory B cells were studied 4 weeks after rAd5 boost. (B) Plasma Ab binding (AUC, area under the curve) to VRC-A, VRC-B (B.HxB2/BaI), and VRC-C (C.97ZA012) HIV-1 gp120 proteins and B.MN gp41 proteins in 4 neonatal (red) and 4 adult (blue) RMs at 4 weeks after rAd5 boost using the BAMA assay. Each symbol represents one animal. (C) Plasma antibody binding (mean) kinetics in DNA/rAd5-vaccinated RMs at 2 weeks after each DNA prime and 4 weeks after rAd5 boost using ELISA. The arrow represents the time of immunization. (D) Plasma samples from DNA/rAd5-vaccinated adult and neonatal RMs were screened for a panel of autologous and heterologous virus isolates via TZM-bl assay. Murine leukemia virus (MuLV) was used as control. The neutralization key is shown at the bottom.

adult RMs (Fig. 1D). Similar to the human HVTN trials with the DNA/rAd5 vaccine, no difficult-to-neutralize (tier 2) virus plasma neutralization activity was observed for either adult or neonatal groups (6).

Analysis of vaccine-induced memory B cell repertoires. Next, we performed single memory B cell sorting by flow cytometry. Vaccine Env VRC-A (A.92RW020) gp140 and a consensus group M (CON-S) gp140 Env were used as fluorophore-labeled recombinant proteins to identify Env-specific memory B cells present in peripheral blood mononuclear cells (PBMCs) of neonatal and adult RMs 4 weeks after final vaccination as described previously (6). MAbs produced from blood IgD⁻ memory B cells of RMs were assayed for binding to autologous HIV-1 Env gp120, gp140, and HIV-1 MN gp41 proteins. For our study, we defined gp120-reactive MAbs as those binding both Env gp140 and gp120 recombinant proteins and gp41-reactive MAbs as those binding recombinant MN gp41 protein or binding to CON-S and/or VRC-A gp140 Envs but not to their autologous gp120 counterparts as described previously (6).

We analyzed 151 HIV-1 Env-reactive MAbs from neonates and 39 HIV-1 Env-reactive MAbs from adults in Env enzyme-linked immunosorbent assay (ELISA) (Fig. 2A). In both cases, the dominant Ab specificity was to gp41 (83% gp41-reactive and 17% gp120-reactive in neonates; 92% gp41-reactive and 8% gp120-reactive in adults), similar to data seen in human trials using the DNA/rAd5 vaccine (Fig. 2A). The results were also the same when we analyzed numbers of unique V_HDJ_H rearrangements that represent the clonal lineages of MAbs. We found that 88% of the 86 unique V_HDJ_H rearrangements in neonates and 92% of the 25 unique heavy-chain sequences in adults induced by the vaccine were gp41 reactive (Fig. 2B). gp41-reactive and gp120-reactive MAbs had similar mean immunoglobulin heavy-chain variable region (IGHV) nucleotide mutation frequencies ($P = 0.781$; sign test) and heavy-chain complementarity-determining region 3 (HCDR3) lengths ($P = 0.156$; sign test) (Fig. 2C and D). Regarding light-chain usage, the vaccine-induced gp41-reactive MAbs used predominantly V κ 1 genes, while gp120-reactive MAbs used predominantly V κ 2 genes (Fig. 2E).

We next asked if the lack of gp120-reactive MAbs was due to an artifact of sorting with gp140 fluorophore-labeled Env proteins. That is, if we had used gp120 fluorophore-labeled proteins to decorate memory B cells, would we have labeled as many gp120-reactive memory B cells as gp41-reactive memory B cells? We compared the flow cytometric staining of memory B cells using fluorophore-labeled CON-S and VRC-A gp120 Envs with that of fluorophore-labeled gp140 Envs for 8 RMs. We found in both cases that the number of gp120-reactive memory B cells was significantly lower than the number of gp140-reactive memory B cells (Fig. 3). We found that VRC-A gp120 bound to 0.11% of memory B cells compared with 0.67% of memory B cells by VRC-A gp140 (mean frequency; $P = 0.016$; Wilcoxon signed-rank test). Similarly, CON-S gp120 bound to 0.08% memory B cells, in comparison with 0.97% by CON-S gp140 (mean frequency; $P = 0.016$; Wilcoxon signed-rank test). Thus, the dearth of isolated gp120-reactive MAbs was mirrored by low frequencies of gp120-reactive memory B cells in the blood of RMs and was not an artifact of gp140 fluorophore-labeled sorting of memory B cells.

Cross-reactivity of vaccine-induced gp41-reactive and gp120-reactive MAbs with fecal bacterial antigens. In HIV-1-infected and Env-vaccinated individuals, gp41-reactive Ab responses developed from preexisting B cells that can cross-react with intestinal microbiota (2, 3, 6). In this study, we first examined the intestinal microbiota composition of RMs by 16S rRNA analysis of vaccinated macaque fecal samples. The fecal microbiota composition of neonatal RMs at the first collection time was not significantly different from that of the mothers (dams) after birth, controlling for the neonate-dam pairing ($P = 0.625$; permutational multivariate analysis of variance [PERMANOVA]) (Fig. 4A). *Streptococcus* was abundant in both neonatal and dam fecal samples at early time points. Alpha diversity was also not significantly different between dams (Shannon index, 4.00 ± 1.00) and neonatal RMs (Shannon index, 4.00 ± 0.91) throughout the experimental time frame ($P = 0.54$; Wilcoxon rank sum test). Early (2 to 4 weeks) and late (>4 weeks) composition differences were identified between

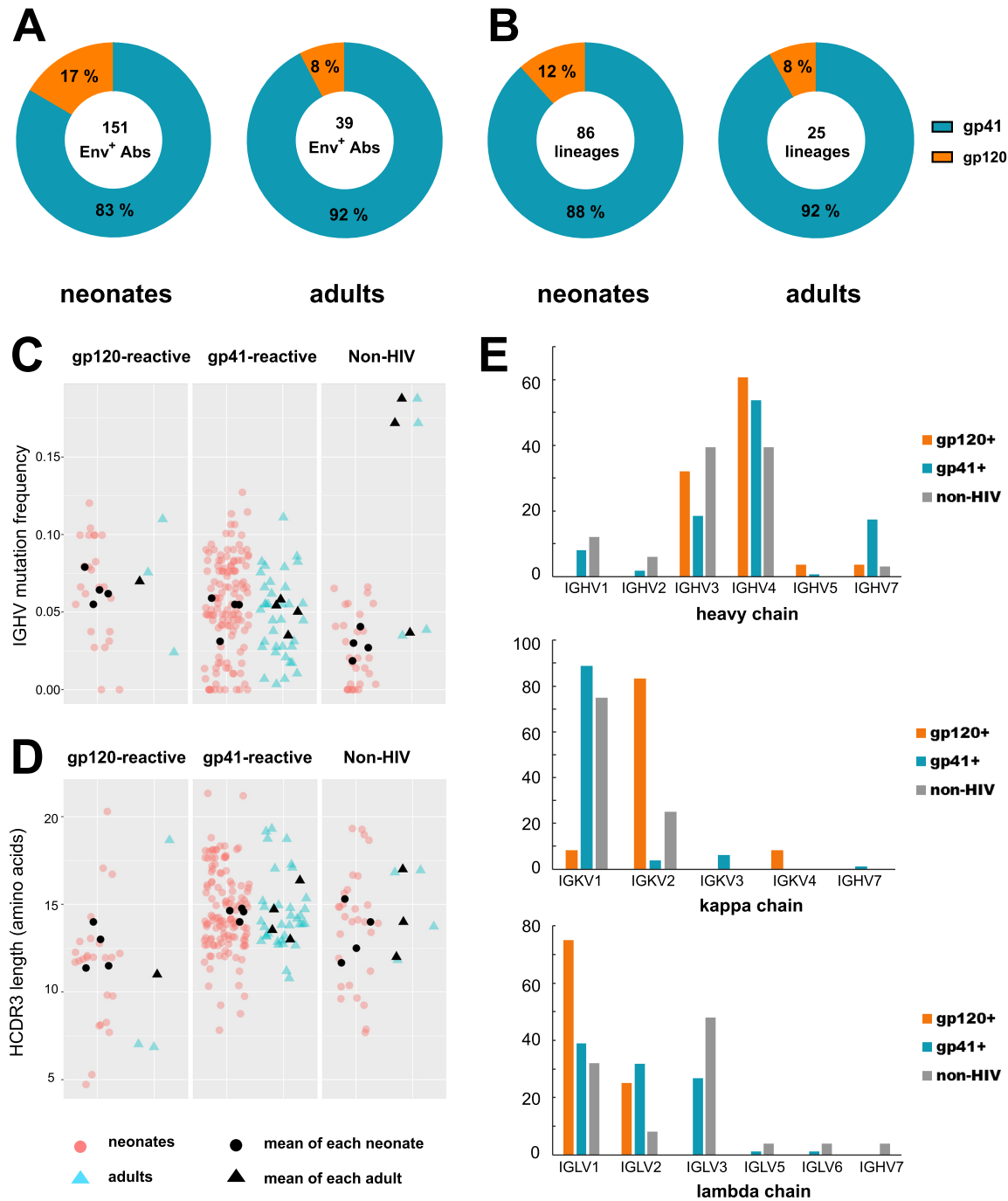
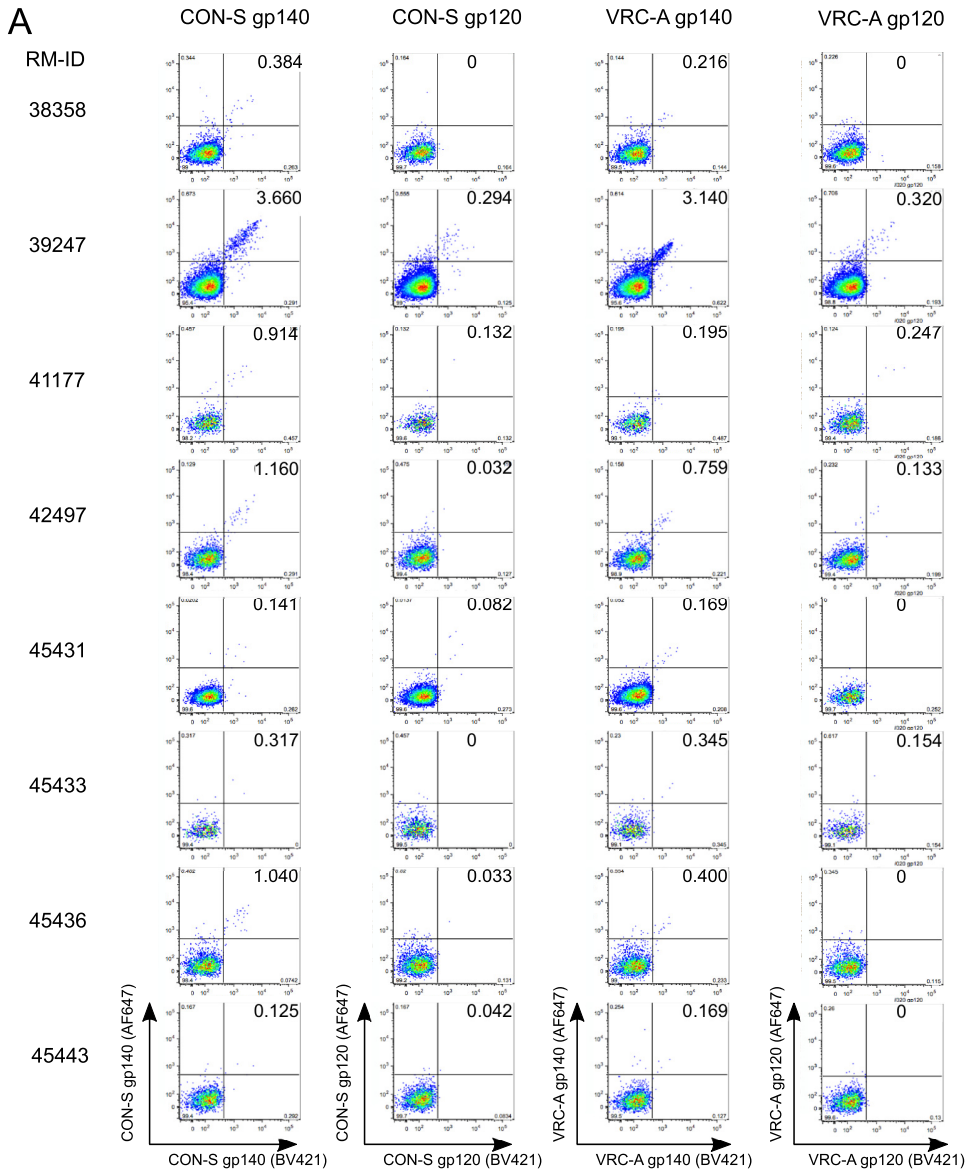


FIG 2 Blood memory B cell repertoire of DNA/rAd5-vaccinated RMs. (A) HIV-1-reactive MAbs were isolated from single memory B cells of neonatal and adult RMs and assayed for binding gp120 and gp41 proteins by ELISA. The percentages of MAb binding to gp41 (teal) and gp120 (orange) are indicated in the pie charts. The total numbers of MAbs generated from neonatal and adult RMs are indicated in the centers of the pie chart. (B) When only unique V_HDJ_H rearrangements were considered, the dominant specificity was still gp41 reactive. The total numbers of unique V_HDJ_H rearrangements generated from neonatal and adult RMs are indicated in the centers of the pie charts. (C and D) The IGHV nucleotide mutation frequency (percent) (C) and amino acid HCDR3 length (D) of gp41-reactive, gp120-reactive, and non-HIV-1 MAbs from neonatal and adult RMs inferred by the Clonality software program. Each symbol represents one MAb, and symbols are color coded for each study: neonatal RMs (red) and adult RMs (blue). The black symbols represent the mean IGHV mutation frequency and HCDR3 length for each RM per study. (E) Distribution of IGHV, IGKV, and IGLV gene families for MAbs isolated from DNA/rAd5-vaccinated RMs. Heavy-chain genes were statistically inferred for 162 gp41-reactive, 28 gp120-reactive, and 33 non-HIV-1-reactive MAbs. Kappa light-chain genes were statistically inferred for 80 gp41-reactive, 24 gp120-reactive, and 8 non-HIV-1-reactive MAbs. Lambda light-chain genes were statistically inferred for 82 gp41-reactive, 4 gp120-reactive, and 25 non-HIV-1-reactive MAbs.



B

RM-ID	CON-S gp140	CON-S gp120	VRC-A gp140	VRC-A gp120
38358	0.384	0	0.216	0
39247	3.660	0.294	3.140	0.320
41177	0.914	0.132	0.195	0.247
42497	1.160	0.032	0.759	0.133
45431	0.141	0.082	0.169	0
45433	0.317	0	0.345	0.154
45436	1.040	0.033	0.400	0
45443	0.125	0.042	0.169	0
Mean % Env positive memory B cells (n=8 RMs)	0.97	0.08	0.67	0.11
Env positive cells: gp140 vs gp120	p=0.016*		p=0.016*	
*Wilcoxon Signed-Rank test				

FIG 3 Flow cytometric staining of blood memory B cells using fluorophore-labeled CON-S and VRC-A gp120 Envs compared with fluorophore-labeled gp140 Envs. (A) Flow plots of gp140 and gp120 (CON-S or VRC-A) staining of Env-reactive memory B cells in 4 neonatal RMs and 4 adult RMs. Memory B cells which bound both BV421-labeled (Continued on next page)

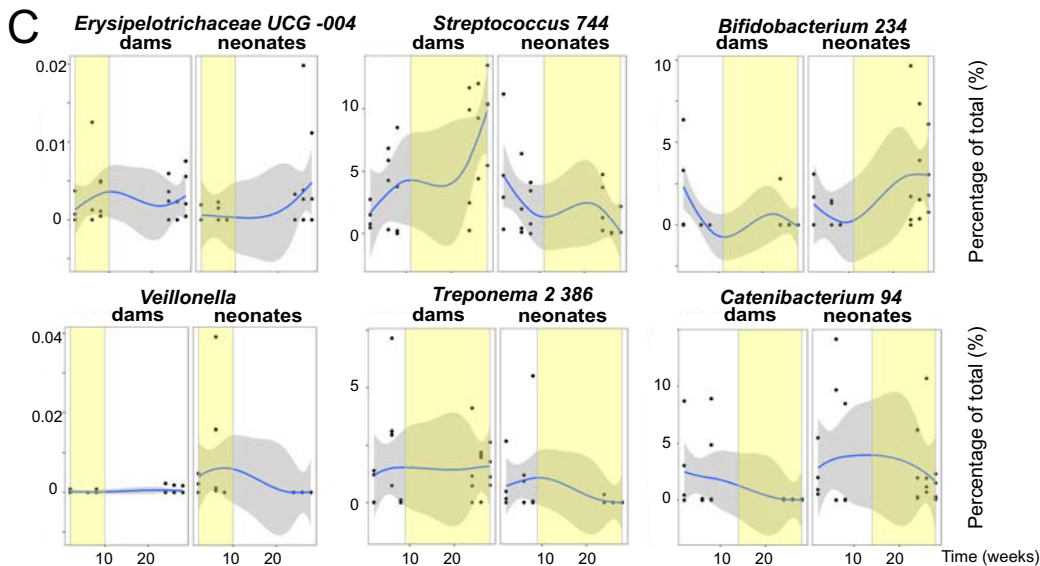
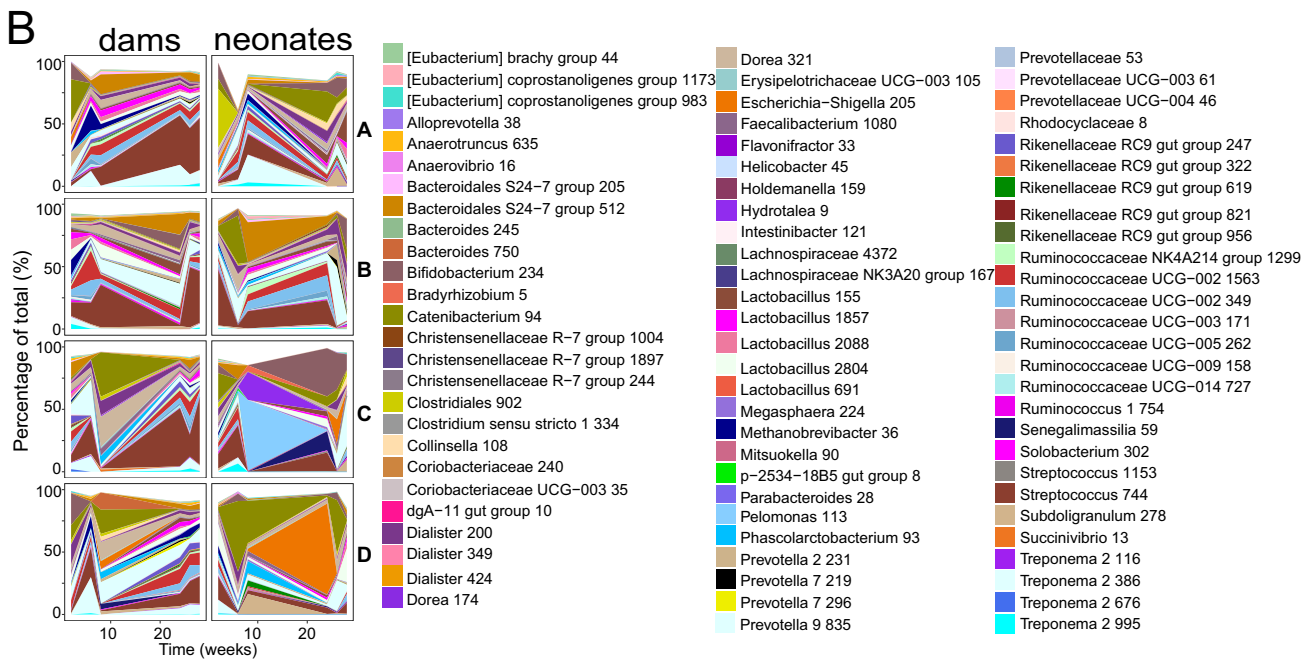
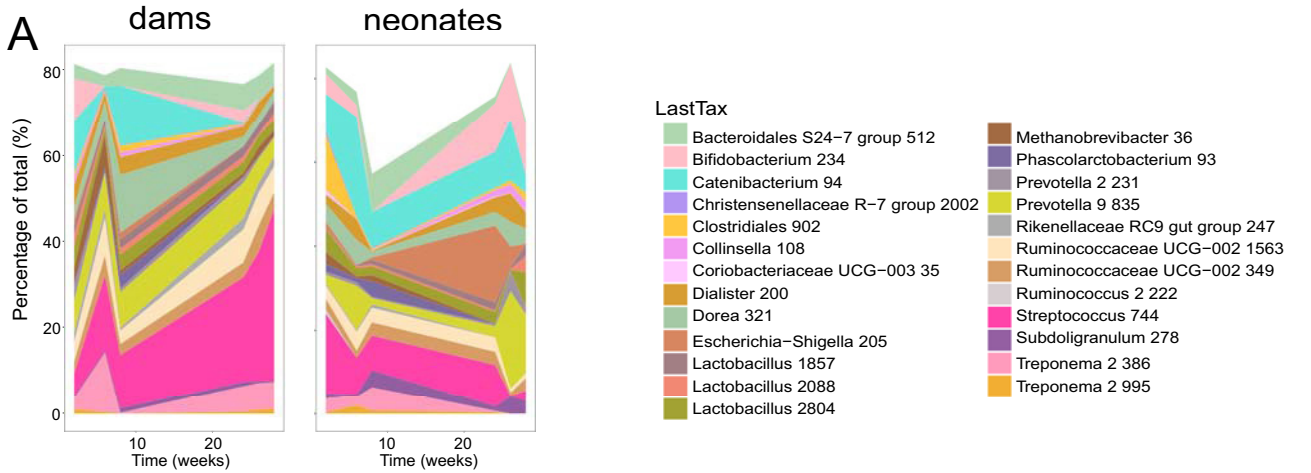
dams and their neonate pairs by smoothing spline ANOVA (Fig. 4). In the early fecal samples, *Prevotella* ($P = 0.029$), *Slackia* ($P = 0.03$), *Erysipelotrichaceae* UCG-004 ($P = 0.012$), and *Lactobacillus* ($P = 0.024$) were more abundant in dam samples, while *Veillonella* ($P = 0.027$) and *Quinella* ($P = 0.001$) were among organisms more abundant in neonatal fecal samples than dam samples (Fig. 4C). Among the multiple late differences in the dam and neonatal RM microbiota were *Streptococcus* (dam > neonate; $P = 0.011$), *Treponema* (dam > neonate; $P = 0.013$), *Bifidobacterium* (neonate > dam; $P = 0.006$), and *Catenibacterium* (neonate > dam; $P = 0.015$) (Fig. 4C).

In human bacterial culture whole-cell lysates (WCLs), two of the candidate gp41-microbiota cross-reactive antigens were bacterial RNA polymerase (*Escherichia coli*) and pyruvate-flavodoxin oxidoreductase (*Megasphaera elsdenii*), which had a sequence similar to LLRAIE (amino acids 555 to 560) of the gp41 heptad repeat 1 region (6). We have previously shown that human gp41-reactive MAb 558_2 cross-reacted with the amino acid sequence NALRAIL of bacterial RNA polymerase and human gp41-reactive MAbs DH438, DH440, and DH432 cross-reacted with a similar sequence, LLRGIK, of pyruvate-flavodoxin oxidoreductase (6). We asked if these cross-reactive epitopes existed in macaque intestinal microbiota. We determined if human gp41-reactive MAbs were cross-reactive with macaque fecal bacterial culture WCLs and found that, indeed, gp41 MAbs from HIV-1-infected or Env-vaccinated individuals bound bacterial proteins of macaque fecal bacterial culture WCLs (Fig. 5A). These data demonstrated that human gp41-reactive MAbs could cross-react with protein(s) in macaque intestinal microbiota. Interestingly, we found in RM fecal samples the presence of *Escherichia* and *Megasphaera* that have BLASTp hits of the LLRAIE sequence by 16S rRNA sequencing (Fig. 5B)—candidates for the observed cross-reactivity of human gp41 MAbs with macaque bacterial antigens. To directly test if the gp41 cross-reactive epitope existed in the intestinal microbiota of neonatal and adult RMs, we performed nested PCR to amplify the DNA sequence encoding cross-reactive epitope from fecal DNA samples. The cross-reactive epitope of amino acids NALRAIL of bacterial RNA polymerase was detected both at the time of the first immunization (0 week) and at 4 weeks after rAd5 boost (28 weeks) in all neonatal and adult RMs we examined (Fig. 5C and D). In neonatal RMs, we detected the presence of amino acids NALRAIL at the earliest time point (0 week: 5 days after birth for neonate 45436 and 6 days after birth for neonate 45433) when the fecal samples were first collected (Fig. 5D). Thus, colonization of the neonate RM gut by bacteria that contained the gp41 cross-reactive epitope of amino acids NALRAIL occurred early after birth.

Next, we asked if macaque gp41-reactive or gp120-reactive MAbs were reactive with their autologous fecal bacterial WCLs. We chose 14 gp41-reactive (representing 13 clonal lineages) and 10 gp120-reactive (representing 10 clonal lineages) macaque MAbs for recombinant Ab production and characterization (Table 1). Five (3 gp41-reactive and 2 gp120-reactive MAbs) of these MAbs were from vaccinated adults and 19 (11 gp41-reactive and 8 gp120-reactive MAbs) were from vaccinated neonates. We used autologous anaerobic and aerobic bacterial WCLs from each RM's fecal culture for Western blot analysis. For the entire group of gp41-reactive and gp120-reactive MAbs, an equal number of MAbs were reactive with autologous fecal bacterial WCLs, ~40% for both groups (Fig. 6A and Tables 2 and 3). None of the gp41-reactive MAbs mediated neutralization against a panel of pseudotyped tier 1 and tier 2 HIV-1 isolates (Fig. 6B). In contrast, 50% (5/10) of vaccine-induced gp120 MAbs neutralized at least 1 HIV-1 isolate in the panel (Fig. 6B). Finally, we examined the polyreactivity of these HIV-1-reactive MAbs by assaying their binding to non-HIV-1 antigens (20, 21). Of the gp41-reactive MAbs, 21% reacted with ≥ 1 of 9 non-HIV-1 host proteins and nucleic acids and 7% reacted with non-HIV-1-infected cells (HEp-2 cells) in an immunofluorescence

FIG 3 Legend (Continued)

Envs (x axis) and AF647-labeled Envs (y axis) were defined as double positive Env-reactive memory B cells. (B) Table showing the frequencies of double positive Env-reactive memory B cells in each RM and the mean frequencies of the 8 RMs. For statistics, the Wilcoxon signed-rank test was used.



reactivity assay (Fig. 6C and Table 2). Of the gp120-reactive MAbs, 20% were reactive with ≥ 1 of 9 host proteins and nucleic acids and 10% reacted with HEp-2 cells (Fig. 6C and Table 2). Thus, similar percentages of vaccine-induced macaque gp41-reactive and gp120-reactive MAbs were polyreactive (Table 3).

DISCUSSION

In this study, we found that the DNA/rAd5 trivalent Env vaccine that induced a gp41 immunodominant Ab response in humans also did so in RMs, as determined by single memory B cell repertoire analysis. In DNA/rAd5-vaccinated neonatal and adult RMs, the majority of anti-HIV-1 Ab specificities of blood memory B cells were gp41 reactive. In contrast, the gp41-reactive plasma Ab response was not significantly different from the gp120-reactive plasma Ab response. Since the plasma binding reflects the sum of the multiple Ab specificities produced by plasmablast/plasma cells, a direct measure of the ratio of gp41-reactive to gp120-reactive Ab levels in plasma is not always a direct measure of the memory B cell repertoire. Thus, an appropriate strategy for analysis of whether new immunogens induce gp41 dominance is to study the memory B cell repertoire. We also noted that neonatal RMs had better neutralizing Ab responses, with higher neutralization titers and better response rates, than adult RMs. Other studies demonstrated that the induction of broadly neutralizing antibodies in HIV-1-infected infants occurs at least as commonly as in adults, and with faster kinetics than in adults (22, 23). The mechanism of better responses in infants compared with adults remains unclear.

Microbial colonization of the gut is a complex multistep process that can imprint both the CD4⁺ T cells and B cell pools of cells (12–16). In our 16S rRNA analysis, the fecal microbiota composition of a neonatal RM at the first sampling time point after birth was similar to that of its mother, demonstrating the rapid influence of the maternal microbiota on colonization of the neonatal gut. *Streptococcus* was among the first abundant colonizers of the intestines of the neonatal RMs in our study. *Streptococcus* organisms are facultative anaerobes, and these bacteria decrease the oxidation potential and facilitate the growth of obligate anaerobes such as *Bifidobacterium* (24–27). Several organisms with abundance differences between neonates and dams were identified at early time points, perhaps resulting from opportunistic colonization of the neonatal gut from environmental exposures. At later time points, we demonstrated the presence of major taxa in the fecal microbiota of both neonatal and adult RMs, such as *Bifidobacterium*, *Streptococcus*, and *Catenibacterium*, which were also found in humans (28–33). *Treponema* was identified in the fecal microbiota of RMs in our study, consistent with a previous study showing that *Treponema* was one of the taxa abundant in the macaque gut microbiota but generally absent in samples from humans (34). The human microbiota composition within the first year of life is less stable, with low diversity and high variations among individuals, compared with the more adult-like intestinal microbiota in humans by 3 years of age (35, 36). In our nonhuman primate model, we found similar alpha diversity between dams and neonatal RMs but time-dependent variation in composition. Primary B cell development in the intestine was shown to be regulated by extracellular signals from the intestinal microbiota (16), which may allow both luminal antigens and peripheral host mucosal components opportunities to influence the preimmune repertoire. In this study, similar to adult RMs, DNA/rAd5-vaccinated neonatal RMs showed dominant gp41-reactive memory B cells in the blood, some of which reacted with intestinal microbiota. One

FIG 4 Changes in the fecal microbial communities of neonatal RMs and dams over time. (A) Changes in the relative proportion of the 25 most abundant assigned taxa over time in neonatal RMs and dams as groups by 16S rRNA sequencing. The lowest meaningful taxonomic assignment (“LastTax”) is shown for each OTU. Taxa were agglomerated using single-linkage phylogenetic clustering at h (cutoff height of the hierarchically clustered phylogenetic tree where organisms with a cophenetic distance smaller than h are agglomerated into one taxon) of 0.2. (B) Relative proportions of the 80 most abundant assigned taxa over time in individual pairs of RM dams and neonates (pairs A to D) by 16S rRNA sequencing. (C) Representative taxon changes over time with windows of statistical differences (yellow) between dams and neonates, controlling for dam-neonate pairs and multiple intraindividual testing using smoothing spline ANOVA. The gray area indicates the confidence intervals, and the blue line indicates the mean percentage of each group. The x axis represents time, in weeks. Each dot represents one animal.

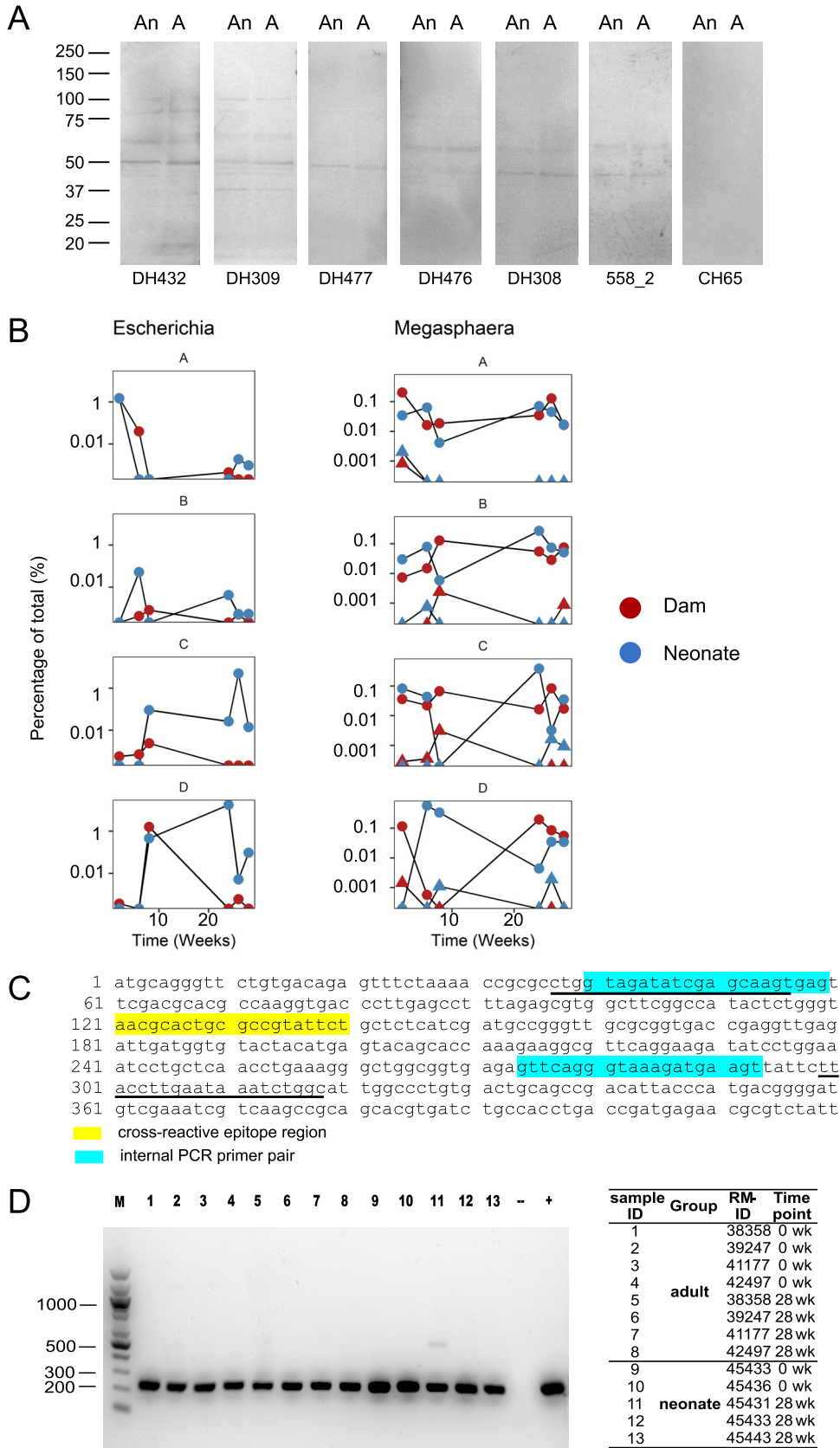


FIG 5 gp41-microbiota cross-reactive epitope existed in the intestinal microbiota of neonatal and adult RMs. (A) Reactivity of human gp41-reactive Abs with macaque fecal anaerobic (An) and aerobic (A) bacterial WCLs tested by SDS-PAGE Western blotting under both nonreducing and reducing conditions (reducing gel is shown). Fifty (Continued on next page)

TABLE 1 Immunogenetics of selected vaccine-induced 14 HIV-1 gp41-reactive MAbs representing 13 clonal lineages and 10 gp120-reactive MAbs representing 10 clonal lineages which were generated as purified MAbs via large-scale transfection^a

MAb ID	Specificity	VH	DH	JH	VH mutation	HCDR3		VL	JL	VL mutation	LCDR3	RM ID
					(%, nt)	length (aa)	(%, nt)			length (aa)		
DH782	gp41	IGHV3-S	IGHD2-11	IGHJ6-1	6.8	15	IGLV1-D	IGLJ2-2	4.5	12	45431	
DH783	gp41	IGHV4-F	IGHD5C-18	IGHJ1-1	4.8	21	IGKV1-S6	IGKJ4-LC1	6.1	9	45431	
DH785	gp41	IGHV1-E	IGHD6-10	IGHJ4-1	0.7	15	IGLV1-B	IGLJ2-2	6.4	10	45431	
DH786	gp41	IGHV7-B	IGHD2C-20	IGHJ5-1	4.9	13	IGLV3-J	IGLJ2-2	7.3	11	45431	
DH787	gp41	IGHV3-Y	IGHD3-21	IGHJ5-1	7.8	13	IGLV2-F	IGLJ2-2	4.1	10	45436	
DH788	gp41	IGHV4-F	IGHD2-13	IGHJ4-1	9.3	16	IGKV1-S7	IGKJ3-2	6.4	9	45436	
DH789	gp41	IGHV4-L	IGHD3-12	IGHJ4-1	8.3	14	IGKV1-S8	IGKJ3-2	12.9	9	45436	
DH790	gp41	IGHV4-E	IGHD1-3	IGHJ4-1	8.9	17	IGKV3-9	IGKJ2-4	1.9	8	45433	
DH791	gp41	IGHV1-E	IGHD4-17	IGHJ2-1	7.7	13	IGLV2-D	IGLJ1-LC1	5.6	9	45433	
DH792	gp41	IGHV1-E	IGHD1-8	IGHJ5-1	8.7	12	IGLV11-A	IGLJ2-2	3.8	10	45443	
DH793	gp41	IGHV4-L	IGHD7-23	IGHJ4-1	8.0	13	IGKV1-15	IGKJ1-5	2.7	9	45443	
DH794	gp41	IGHV4-F	IGHD2-13	IGHJ4-1	8.2	14	IGLV2-D	IGLJ1-LC1	4.8	10	41177	
DH795.1	gp41	IGHV4-H	IGHD1-8	IGHJ4-1	4.5	15	IGLV2-E	IGLJ1-LC1	4.1	11	41177	
DH795.2	gp41	IGHV4-H	IGHD1-8	IGHJ4-1	7.6	15	IGLV2-E	IGLJ1-LC1	3.0	11	41177	
DH796	gp120	IGHV4-I	IGHD4C-17	IGHJ5-1	10.0	12	IGKV2-S20	IGKJ3-2	2.1	9	45431	
DH797	gp120	IGHV3-L	IGHD2-16	IGHJ4-1	3.1	5	IGKV2-S10	IGKJ3-2	8.6	9	45431	
DH798	gp120	IGHV3-AA	IGHD6-19	IGHJ4-1	3.7	8	IGKV2-S18	IGKJ2-4	1.4	9	45431	
DH799	gp120	IGHV5-A	IGHD3C-12	IGHJ6-1	0.0	20	IGKV1-22	IGKJ2-4	3.4	9	45431	
DH800	gp120	IGHV4-K	IGHD4-17	IGHJ1-1	7.9	13	IGLV1-F	IGLJ1-LC1	3.4	11	45436	
DH801	gp120	IGHV3-Q	IGHD6-15	IGHJ2-1	6.6	10	IGKV4-3	IGKJ2-4	4.3	9	45436	
DH802	gp120	IGHV4-H	IGHD3-12	IGHJ4-1	5.5	13	IGLV1-F	IGLJ6-LC1	3.4	11	45433	
DH803	gp120	IGHV4-J	IGHD4-22	IGHJ4-1	6.2	14	IGKV2-S12	IGKJ4-LC1	2.5	9	45443	
DH804	gp120	IGHV4-J	IGHD2-20	IGHJ5-1	2.4	19	IGKV2-S20	IGKJ4-LC1	6.0	9	41177	
DH805	gp120	IGHV4-D	IGHD7-23	IGHJ5-1	7.6	7	IGKV2-S17	IGKJ1-5	3.9	9	41177	

^aHeavy chain V (VH), D (DH), J (JH) segment, VH mutation frequency, HCDR3 length, light chain V (VL), J (JL) gene usage, VL mutation frequency, and LCDR3 length are shown. aa, amino acids.

possible explanation is that the expansion of the intestinal microbiota occurred sufficiently early in neonatal RMs (3.8 days after birth) to shape the B cell repertoire in neonatal RMs before the B cell repertoire could be imprinted by other neutralizing or subdominant gp120 Env antigenic sites. Indeed, we demonstrated that the cross-reactive sequence NALRAIL of bacterial RNA polymerase was present by the time the first samples were taken in neonatal RMs, at 5 (RM45436) or 6 (RM45433) days after birth. It will be of interest to determine if earlier or intrauterine immunization of fetal RMs can alter the Env-reactive repertoire.

In summary, our results suggest that the RM model can be used to study the question of gp41 dominance induced by new Env-containing HIV-1 experimental immunogens, provided that the memory B cell repertoire is probed. Future studies of HIV-1 Env designs should consider deleting or modifying regions of gp41 that are cross-reactive with microbiota to avoid dominant nonneutralizing gp41 responses.

FIG 5 Legend (Continued)

micrograms of anaerobic and aerobic bacterial WCLs was loaded in individual lanes, and MAbs were tested at 20 μ g/ml. DH432, DH477, and DH476 were from HVTN505 (6), DH308 and DH309 were from chronically HIV-1-infected individuals (3), and 558_2 was from acutely HIV-1-infected individuals (2). CH65 (anti-influenza virus) MAb was used as a negative control. (B) Changes in the relative proportions of assigned taxa *Escherichia-Shigella* and *Megasphaera* over time in individual neonatal RMs (blue, A to D) and dams (red, A to D) by 16S rRNA sequencing. One assigned taxon for *Escherichia-Shigella* (*Escherichia-Shigella* 205) and two assigned taxa for *Megasphaera* are shown (circles, *Megasphaera* 224; triangles, *Megasphaera* 35). The x axis represents time, in weeks. (C) Design of nested PCR amplifying the cross-reactive sequence NALRAIL of bacterial RNA polymerase. The yellow region indicates the cross-reactive epitope NALRAIL sequence. Sequences of external PCR primers are underlined; the blue region indicates the locations of internal PCR primers. GenBank accession number for protein sequence, [WP_001162094.1](#) (DNA-directed RNA polymerase subunit alpha); GenBank accession number for nucleotide sequence, [NZ_CP014070.1](#) (region: reverse complement 82961.0.83950). (D) Nested PCR amplifying the cross-reactive epitope NALRAIL of bacterial RNA polymerase in equal amounts (60 ng) of fecal DNA from neonatal and adult RMs. Gel electrophoresis of nested PCR amplicons is shown. The sample identifier (ID), group, RM ID, and time point information are listed on the right. M, 100-bp DNA markers; -, negative control PCR without DNA template (blank control); +, positive control PCR using 60 ng genomic DNA extracted from *E. coli* as the template. Another negative control was used for the DNA extraction (molecular-grade water instead of fecal sample), but data are not shown.

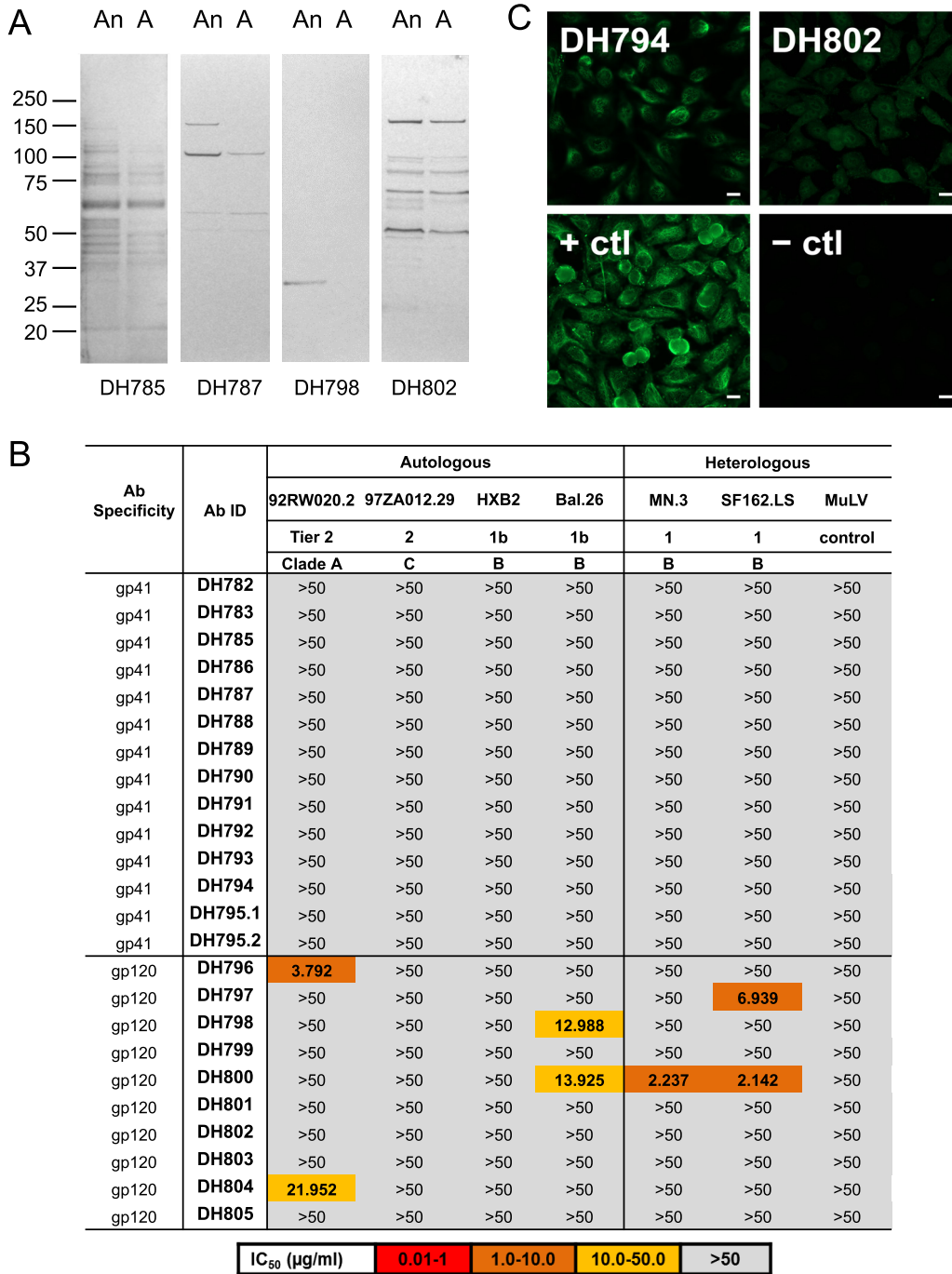


FIG 6 Polyreactivity of vaccine-induced gp41-reactive and gp120-reactive MAbs in DNA/rAd5-vaccinated RMs. (A) Cross-reactivities of representative gp41-reactive (DH785 and DH787) and gp120-reactive (DH798 and DH802) MAbs isolated from blood memory B cells of DNA/rAd5-vaccinated RMs against autologous anaerobic (An) and aerobic (A) fecal bacterial WCLs by SDS-PAGE Western blotting. A total of 50 μ g each of anaerobic and aerobic bacterial WCLs was loaded in individual lanes, and MAbs were tested at 20 μ g/ml under both nonreducing and reducing conditions. Examples of Western blots of macaque Env MAbs under reducing conditions are shown. (B) Neutralization profile of HIV-1 gp41-reactive and gp120-reactive MAbs. Env-reactive MAbs were screened for HIV-1 neutralization via a TZM-bl assay. The control virus was murine leukemia virus (MuLV). The neutralization color key is shown at the bottom. (C) HEP-2 epithelial cells were stained with gp41-reactive (DH794) and gp120-reactive (DH802) MAbs at a concentration of 50 μ g/ml, followed by incubation with FITC-labeled goat anti-human Ab. Images were acquired for 8 or 12 s (DH794 and DH802). + ctl, MAb Ab901062Rh (gp41); - ctl, DH570.30 (gp41). Scale bars, 25 μ m. Data are representative of results from at least two separate experiments.

TABLE 2 Polyreactivities of vaccine-induced gp41-reactive and gp120-reactive MAbs from DNA/rAd5-vaccinated RMs^a

MAb ID	Specificity	Anaerobe WCL reactivity	Aerobe WCL reactivity	Autoantigen binding by ELISA	HEp-2 cell reactivity
DH782	gp41	–	–	RNP	–
DH783	gp41	–	–	–	–
DH785	gp41	+	+	RNP	–
DH786	gp41	–	–	–	–
DH787	gp41	+	+	–	–
DH788	gp41	–	–	–	–
DH789	gp41	–	–	–	–
DH790	gp41	–	–	Histone	–
DH791	gp41	–	–	–	–
DH792	gp41	+	+	–	–
DH793	gp41	–	–	–	–
DH794	gp41	+	–	–	Cytoskeletal, perinuclear coil, vimentin
DH795.1	gp41	+	+	–	–
DH795.2	gp41	+	+	–	–
DH796	gp120	–	–	Histone	–
DH797	gp120	–	–	–	–
DH798	gp120	+	–	–	–
DH799	gp120	–	–	–	–
DH800	gp120	–	–	–	–
DH801	gp120	+	+	–	–
DH802	gp120	+	+	SSA, SSB, Scl-70, Sm, RNP	Nuclear +, cytoplasmic +, surface + (rim), nucleoli –
DH803	gp120	–	–	–	–
DH804	gp120	–	–	–	–
DH805	gp120	+	+	–	–

^aMAbs were assayed for cross-reactivity with anaerobic and aerobic bacterial WCLs of autologous macaque fecal samples, host antigens (autoantigens binding by ELISA), and HEp-2 cells (indirect fluorescence antibody assay [IFA]; Zeus Scientific).

MATERIALS AND METHODS

Animals, vaccine, and procedures. All rhesus macaques (*Macaca mulatta*) were housed indoors at the California National Primate Research Center (CNPRC) and were maintained in accordance with the Association for Assessment and Accreditation of Laboratory Animals with the approval of the Animal Care and Use Committees of the UC Davis. Research was conducted in compliance with the Animal Welfare Act and other federal statutes and regulations relating to animals and experiments involving animals and adhered to principles stated in the *Guide for the Care and Use of Laboratory Animals* (37). The neonatal RMs were dam-reared and were up to 6 days of age at the time of the first immunization. Dam-reared neonates were selected because dam-rearing is most natural and because it was previously shown that nursery-reared infants have differences in microbiome and immune function (38, 39). The 4 adult animals were 3 to 8 years old at enrollment. When necessary, adult animals were immobilized with ketamine hydrochloride (10 mg/kg of body weight) administered intramuscularly; when feasible, neonatal RMs were handheld for the procedures and sample collections. Blood samples were collected via venipuncture. Stool was collected from the cage pan, or from the neonatal RMs when they were handheld.

TABLE 3 Percentages of polyreactive vaccine-induced gp41-reactive and gp120-reactive MAbs from DNA/rAd5-vaccinated RMs^a

Antigen	No. of polyreactive MAbs/total no. of gp41-reactive MAbs (%)	No. of polyreactive MAbs/total no. of gp120-reactive MAbs (%)
Anaerobe WCLs	6/14 (43)	4/10 (40)
Aerobe WCLs	5/14 (36)	3/10 (30)
Autoantigens (ELISA)	3/14 (21)	2/10 (20)
HEp-2 cells (IFA)	1/14 (7)	1/10 (10)

^aSee footnote *a* to Tables 2 for details. The *P* values, generated by means of Fisher's exact test (SAS v9.4), were 1 in all cases.

The 6-plasmid DNA vaccine (expressing HIV-1 *gag*, *pol*, and *nef* genes as well as a trivalent mixture of clade A, B, and C *env* gp145 genes) was administered via the intramuscular route at weeks 0, 4, and 8, and the rAd5 vector boost (expressing clade B Gag-Pol fusion protein and gp140 Env glycoproteins from clades A, B, and C) was administered via the intramuscular route at week 24 (4–6). Blood samples were collected at 2 weeks after each immunization. Vaccine-induced Ab repertoires were studied 4 weeks after rAd5 boost in blood-derived memory B cells of four neonatal RMs and four adult RMs.

Flow cytometry memory B cell single-cell sorting. B cell sorting was performed as described previously (6, 40). Briefly, PBMCs of immunized RMs were stained with AquaVital dye, CD14 (BV570), CD16 (phycoerythrin [PE]-Cy7), CD3 (peridinin chlorophyll protein [PerCP] Cy5.5), CD20 (fluorescein isothiocyanate [FITC]), CD27 (allophycocyanin [APC]-Cy7), and IgD (PE). Single-cell isolation of memory B cells (AquaVital dye⁻, CD14⁻, CD16⁻, CD3⁻, IgD⁻, and CD20⁺) decorated with both Alexa Fluor 647 and brilliant violet 421-tagged VRC-A (A.92RW020) or CON-S Env gp140s (41) was performed using a FACSAria II fluorescence-activated cell sorter (BD Biosciences, San Jose, CA), and the flow cytometry data were analyzed using FlowJo (Treestar, Ashland, OR).

PCR isolation of heavy- and light-chain genes. Heavy-chain (*IGHV*) and light-chain (*IGKV* and *IGLV*) genes were amplified as described previously (42). The PCR-amplified genes were then purified and sequenced with 4 μ M forward and reverse primers. Sequences were analyzed by using the macaque library in Clonality (43) for the VDJ arrangements of the immunoglobulin *IGHV*, *IGKV*, and *IGLV* sequences, mutation frequencies, and CDR3 length (40, 44). Sequences were subject to statistical analysis for lineage membership as described previously (6).

Transient and recombinant antibody expression. Transient and recombinant MAb expressions were performed as previously described (2, 40, 42). Briefly, an aliquot of the purified PCR amplicon was used for overlapping PCR to generate a linear expression cassette. The expression cassette was transfected with ExpiFectamine (Thermo Fisher Scientific) into 293T cells. The supernatant containing recombinant Abs were used for binding assays. The genes of selected heavy chains and kappa/lambda chains were synthesized as IgG1 and cloned into pcDNA3.1 plasmid (GenScript). Recombinant MAb expressions and purification were performed as previously described (2, 40).

Antibody binding. Plasma Abs and recombinant MAbs were assayed for binding specificities to multiclade HIV-1 gp120 Envs and clade B.MN gp41 (product 10911; ImmunoDX, Woburn, MA) by means of standard ELISA as previously described (1, 6). The binding antibody multiplex assay (BAMA) was used to determine reactivity of plasma Abs with antigens as previously described (1).

Neutralization assays. Neutralization activity of plasma Abs and recombinant MAbs was measured in 96-well culture plates by using Tat-regulated luciferase reporter gene expression to quantify reductions in virus infection in TZM-bl cells as previously described (45–48).

Antibody polyreactivity. Bacterial WCLs were prepared as previously described (2, 3, 6). Reactivity with 50- μ g anaerobic or aerobic WCLs of fecal bacterial culture was determined by Western blotting. A 20- μ g/ml concentration of MAbs was used to test reactivity with WCLs. Fecal bacterial WCLs from each RM (RM45436, RM45433, RM45431, RM45443, and RM41177) were used for testing cross-reactivity of gp41 and gp120 MAbs from the corresponding RM. Fecal bacterial WCLs from RM45436 were used for testing the cross-reactivity of human gp41 MAbs. CH65 (anti-influenza virus) MAb was used as a negative control.

Vaccine-induced MAbs were tested for binding autoantigens by ELISA. The ELISA panel consisted of nine autoantigens: Sjogren's syndrome antigen A (SSA), Sjogren's syndrome antigen (SSB), Smith antigen (Sm), ribonucleoprotein (RNP), scleroderma 70 (Scl-70), Jo-1 antigen, double-stranded DNA (dsDNA), centromere B (Cent B), and histone. Direct binding ELISAs were conducted in 384-well ELISA plates (Costar; number 3700) coated with 2 μ g/ml of autoantigens in 0.1 M sodium bicarbonate overnight at 4°C (for dsDNA, the plates were coated with poly-L-lysine and washed, and then 10 μ l of dsDNA diluted to 20 μ g/ml in 1% bovine serum albumin [BSA] in phosphate-buffered saline [PBS]–0.05% Tween 20 was added and incubated at room temperature for 1 h). Plates were washed with PBS–0.05% Tween 20 and blocked with 3% BSA in PBS at room temperature for 1 h. MAb samples were incubated for 45 min in 3-fold serial dilutions beginning at 50 μ g/ml, followed by washing with PBS–0.05% Tween 20. Ten microliters of horseradish peroxidase (HRP)-conjugated goat anti-monkey secondary Ab was diluted to 1:8,000 in 1% BSA in PBS–0.05% Tween 20 and incubated at room temperature for 1 h. These plates were washed four times and developed with tetramethylbenzidine substrate (20 μ l per well) (SureBlue Reserve) for 15 min. The HRP reaction was stopped with 1 M HCl (20 μ l per well), and optical density at 450 nm (OD_{450}) was determined. The positivity cutoff for binding for each autoantigen in the autoreactivity assay was (i) an OD_{450} of ≥ 0.5 , (ii) an OD_{450} that was ≥ 8 times the standard deviation of predetermined background reactivity of 40 MAbs that are not autoreactive, or (iii) at least positive at concentrations of 50 and 16.7 μ g/ml. CH65 (anti-influenza virus) MAb was used as a negative control. Polyclonal human origin plasma against each antigen was used as a positive control.

Indirect immunofluorescence binding of MAbs to HEp-2 cells (Inverness Medical Professional Diagnostics, Princeton, NJ) was determined as described previously (2, 3, 6, 21, 49). Briefly, 20 μ l of MAb at 50 and 25 μ g/ml was placed on a predetermined spot on the surface of an ANA HEp-2 kit slide, incubated for 25 min at room temperature, washed, and developed with 20 μ l of goat anti-monkey Ig-FITC at 20 μ g/ml (Southern Biotech, Birmingham, AL) for 25 min. Incubations were performed in humid chambers in the dark. Slides were then washed and dried; a drop of 33% glycerol was placed on each spot prior to the fixing of coverslips. Images were taken on an Olympus AX70 with a SpotFlex FX1520 charge-coupled device (CCD) with a UPlanFL 40 \times (numerical aperture, 0.75) objective at 25°C in the FITC channel using SPOT software. Images were acquired for 8 s or 12 s. Image layout and scaling were performed in

Adobe Photoshop without image manipulation. MAbs Ab901062Rh (gp41) and DH570.30 (gp41) were used as positive and negative controls, respectively. Reactivity patterns were defined by Zeus Scientific.

Stool DNA extraction, PCR amplification, and DNA sequencing. For nested PCR amplification of cross-reactive epitope, genomic DNA from fecal sample was extracted according to the instructions of the QIAamp DNA stool minikit (Qiagen, Hilden, Germany). For 16S rRNA sequencing, total genomic DNA was extracted from fecal samples using a commercial bead-beating method (Zymo Research Soil Microbe DNA kit, Irvine, CA). PCR amplification of the V4 region of the 16S rRNA gene and gel extraction of the PCR amplicons were performed as previously described (50). Sequencing was performed on the Illumina HiSeq Platform (Illumina, Inc., San Diego, CA) with the use of 150-nucleotide (nt) single-end reads. Sequences were filtered, clustered into operational taxonomic units (OTUs), and aligned to the Greengenes database (version 13.8.99) as previously described (50). Representative sequences of the clusters were assigned to a particular level of taxonomy using BLAST against the SILVA bacterial database (release 111).

Nested PCR. Nested PCR amplifications were performed using iProof DNA polymerase (Bio-Rad). The PCR master mixture of the first-round PCRs included 60 ng of fecal DNA as the template, deoxynucleoside triphosphates (dNTPs) with each at 200 μ M, 0.5 μ l of iProof DNA polymerase, and each primer at 0.5 μ M in a total volume of 50 μ l. The second-round amplifications used 0.5 μ l of the amplicon from the first round PCR as the template in a total volume of 50 μ l. The primer sequences used in the first round PCR were 5'-CTGGTAGATATCGAGCAAGT-3' (forward primer) and 5'-GCCAGATTATTCAAGGTAA-3' (reverse primer), and those in the second round were 5'-GTAGATATCGAGCAAGTGAG-3' (forward primer) and 5'-ACTTCATCTTTACCCCTGAAC-3' (reverse primer). Cycling conditions involved denaturation at 98°C for 30 s, followed by 30 cycles, each consisting of denaturing at 98°C for 10 s, annealing at 57°C for 20 s, and extension at 72°C for 20 s, followed by extension at 72°C for 10 min. PCR products were then stained with SYBR Safe DNA gel stain (Invitrogen), electrophoresed with a 1% agarose gel, and visualized under UV light. Negative controls included one for the PCR (blank control) and another for the DNA extraction (molecular-grade water instead of fecal sample), and the positive control was 60 ng of genomic DNA extracted from *E. coli*. PCR products were purified from a 1% agarose gel with a gel extraction kit (Qiagen), and the sequence was confirmed by DNA sequencing (Genewiz).

Microbial composition and diversity. Microbial composition and diversity were determined by the use of tools within the phyloseq (version 1.14.0), vegan (version 2.4-1), gss (version 2.1-6), and metagenomeSeq (version 1.12.0) packages as previously described (50). All analyses were performed with R statistical software (R Foundation for Statistical Computing, Vienna, Austria). Statistical analysis of neonate versus dam community relatedness was performed using PERMANOVA. Wilcoxon rank sum test was performed to compare the alpha diversity of neonate and dam fecal samples. Analysis of taxon changes overtime with windows of statistical differences between dams and neonates controlling for dam-neonate pairs and multiple intraindividual testing was performed using smoothing spline ANOVA (51). A *P* value of < 0.05 was considered statistically significant, with Benjamini-Hochberg correction for multiple testing.

Statistical analysis. Wilcoxon signed-rank test was performed to compare differences in (i) plasma Ab responses to gp41 and gp120 and (ii) frequencies of gp120-reactive and gp140-reactive memory B cells. Sign test was performed to compare the heavy-chain mutation frequency and HCDR3 length of gp120-reactive and gp41-reactive MAbs. Fisher's exact test was performed to compare the polyreactivity profile of gp120-reactive and gp41-reactive MAbs. Descriptive statistics were used to describe immune responses. Statistics were calculated with SAS v9.4.

Accession number(s). Sequences for the antibodies isolated in this study are available in GenBank (accession numbers [MF535578](#) to [MF535625](#)).

ACKNOWLEDGMENTS

We thank Lawrence Armand for production of fluorophore-labeled reagents; Andrew Foulger, Amanda Eaton, Felix Araujo-Perez, Ryan Mathura, Michelle Key, Meng Chen, Amy Wang, Shi-Mao Xia, Melissa Cooper, Rachel Reed, Giovanna Hernandez, Esther Lee, Erika Dunford, Callie Vivian, Stormi Chadwick, Maggie Barr, and Sabrina Arora for technical assistance; Jennifer Watanabe and Colony Research Services of CNPRC; and the Center for HIV/AIDS Vaccine Immunology and Immunogen Discovery.

Research materials used in this study are available from Duke University upon request and subsequent execution of an appropriate materials transfer agreement.

Research reported in this publication was supported by the NIAID of the NIH and by the Center for HIV/AIDS Vaccine Immunology and Immunogen Discovery (CHAVI-ID; grant number UM1-AI100645), NIH NIAID Duke University Center for AIDS Research (CFAR; P30-AI-64518), the Office of Research Infrastructure Programs/OD (P51OD011107) (to CNPRC), and the intramural research program of the Vaccine Research Center, NIAID, NIH.

Q.H. designed and performed experiments, analyzed data, and cowrote the paper; M.A.M., D.J.M., and J.F.W. performed isolation of Abs; T.B.K., K.J.W., K.O.S., and A.M.T. performed computational analysis of Ab sequences; K.E.S., R.J.P., and M.S.A. performed Ab binding assays; T.V.H. performed HEP-2 cell staining; K.L. and T.C.G. prepared

bacterial whole-cell lysates; L.L.S. and C.B. performed experiment immunizations, analyzed data, and edited the paper; N.V. performed statistical analysis; D.C.M. performed neutralization assays; P.C.S. performed 16S rRNA sequencing and analysis; J.R.M. and B.S.G. provided the DNA/rAd5 vaccine, participated in experimental design, and edited the paper; K.K.A.V.R. participated in experimental design and data analysis, managed the vaccination of the animals and sample collection, and edited the paper; G.D.T., W.B.W., K.O.S., S.R.P., and M.A.M. analyzed data, designed experiments, reviewed data, and edited the paper; and B.F.H. conceived and designed the study, reviewed all data, and cowrote the paper.

REFERENCES

- Tomaras GD, Yates NL, Liu P, Qin L, Fouda GG, Chavez LL, Decamp AC, Parks RJ, Ashley VC, Lucas JT, Cohen M, Eron J, Hicks CB, Liao H-X, Self SG, Landucci G, Forthal DN, Weinhold KJ, Keele BF, Hahn BH, Greenberg ML, Morris L, Karim SSA, Blattner WA, Montefiori DC, Shaw GM, Perelson AS, Haynes BF. 2008. Initial B-cell responses to transmitted human immunodeficiency virus type 1: virion-binding immunoglobulin M (IgM) and IgG antibodies followed by plasma anti-gp41 antibodies with ineffective control of initial viremia. *J Virol* 82:12449–12463. <https://doi.org/10.1128/JVI.01708-08>.
- Liao H-X, Chen X, Munshaw S, Zhang R, Marshall DJ, Vandergrift N, Whitesides JF, Lu X, Yu J-S, Hwang K-K, Gao F, Markowitz M, Heath SL, Bar KJ, Goepfert PA, Montefiori DC, Shaw GC, Alam SM, Margolis DM, Denny TN, Boyd SD, Marshal E, Egholm M, Simen BB, Hanczaruk B, Fire AZ, Voss G, Kelsoe G, Tomaras GD, Moody MA, Kepler TB, Haynes BF. 2011. Initial antibodies binding to HIV-1 gp41 in acutely infected subjects are polyreactive and highly mutated. *J Exp Med* 208:2237–2249. <https://doi.org/10.1084/jem.20110363>.
- Trama AM, Moody MA, Alam SM, Jaeger FH, Lockwood B, Parks R, Lloyd KE, Stolarchuk C, Scarce R, Foulger A, Marshall DJ, Whitesides JF, Jeffries TL, Jr, Wiehe K, Morris L, Lamborn B, Soderberg K, Hwang K-K, Tomaras GD, Vandergrift N, Jackson KJL, Roskin KM, Boyd SD, Kepler TB, Liao H-X, Haynes BF. 2014. HIV-1 envelope gp41 antibodies can originate from terminal ileum B cells that share cross-reactivity with commensal bacteria. *Cell Host Microbe* 16:215–226. <https://doi.org/10.1016/j.chom.2014.07.003>.
- Churchyard GJ, Morgan C, Adams E, Hural J, Graham BS, Moodie Z, Grove D, Gray G, Bekker L-GG, McElrath MJ, Tomaras GD, Goepfert P, Kalams S, Baden LR, Lally M, Dolin R, Blattner W, Kalichman A, Figueroa JP, Pape J, Schechter M, Defawe O, De Rosa SC, Montefiori DC, Nabel GJ, Corey L, Keefer MC, NIAID HIV Vaccine Trials Network. 2011. A phase IIA randomized clinical trial of a multiclade HIV-1 DNA prime followed by a multiclade rAd5 HIV-1 vaccine boost in healthy adults (HVTN204). *PLoS One* 6:e21225. <https://doi.org/10.1371/journal.pone.0021225>.
- Hammer SM, Sobieszczyk ME, Janes H, Karuna ST, Mulligan MJ, Grove D, Koblin BA, Buchbinder SP, Keefer MC, Tomaras GD, Frahm N, Hural J, Anude C, Graham BS, Enama ME, Adams E, DeJesus E, Novak RM, Frank I, Bentley C, Ramirez S, Fu R, Koup RA, Mascola JR, Nabel GJ, Montefiori DC, Kublin J, McElrath MJ, Corey L, Gilbert PB, Team HS. 2013. Efficacy trial of a DNA/rAd5 HIV-1 preventive vaccine. *N Engl J Med* 369:2083–2092. <https://doi.org/10.1056/NEJMoa1310566>.
- Williams WB, Liao H-X, Moody MA, Kepler TB, Alam SM, Gao F, Wiehe K, Trama AM, Jones K, Zhang R, Song H, Marshall DJ, Whitesides JF, Sawatzki K, Hua A, Liu P, Tay MZ, Seaton KE, Shen X, Foulger A, Lloyd KE, Parks R, Pollara J, Ferrari G, Yu J-S, Vandergrift N, Montefiori DC, Sobieszczyk ME, Hammer S, Karuna S, Gilbert P, Grove D, Grunenberg N, McElrath MJ, Mascola JR, Koup RA, Corey L, Nabel GJ, Morgan C, Churchyard G, Maenza J, Keefer M, Graham BS, Baden LR, Tomaras GD, Haynes BF. 2015. Diversion of HIV-1 vaccine-induced immunity by gp41-microbiota cross-reactive antibodies. *Science* 349:aab1253. <https://doi.org/10.1126/science.aab1253>.
- Goepfert PA, Elizaga ML, Seaton K, Tomaras GD, Montefiori DC, Sato A, Hural J, DeRosa SC, Kalams SA, McElrath MJ, Keefer MC, Baden LR, Lama JR, Sanchez J, Mulligan MJ, Buchbinder SP, Hammer SM, Koblin BA, Pensiero M, Butler C, Moss B, Robinson HL, HVTN 205 Study Group, National Institutes of Allergy and Infectious Diseases HIV Vaccines Trials Network. 2014. Specificity and 6-month durability of immune responses induced by DNA and recombinant modified vaccinia Ankara vaccines expressing HIV-1 virus-like particles. *J Infect Dis* 210:99–110. <https://doi.org/10.1093/infdis/jiu003>.
- Liu J, Ghneim K, Sok D, Bosche WJ, Li Y, Chipriano E, Berkemeier B, Oswald K, Borducchi E, Cabral C, Peter L, Brinkman A, Shetty M, Jimenez J, Mondesir J, Lee B, Giglio P, Chandrashekar A, Abbink P, Colantonio A, Gittens C, Baker C, Wagner W, Lewis MG, Li W, Sekaly R-P, Lifson JD, Burton DR, Barouch DH. 2016. Antibody-mediated protection against SHIV challenge includes systemic clearance of distal virus. *Science* 353:1045–1049. <https://doi.org/10.1126/science.aag0491>.
- Barouch DH, Stephenson KE, Borducchi EN, Smith K, Stanley K, McNally AG, Liu J, Abbink P, Maxfield LF, Seaman MS, Dugast AS, Alter G, Ferguson M, Li W, Earl PL, Moss B, Giorgi EE, Szinger JJ, Eller LA, Billings EA, Rao M, Tovanabutra S, Sanders-Buell E, Weijtens M, Pau MG, Schuitemaker H, Robb ML, Kim JH, Korber BT, Michael NL. 2013. Protective efficacy of a global HIV-1 mosaic vaccine against heterologous SHIV challenges in rhesus monkeys. *Cell* 155:531–539. <https://doi.org/10.1016/j.cell.2013.09.061>.
- Shedlock DJ, Silvestri G, Weiner DB. 2009. Monkeying around with HIV vaccines: using rhesus macaques to define “gatekeepers” for clinical trials. *Nat Rev Immunol* 9:717–728. <https://doi.org/10.1038/nri2636>.
- Barouch DH, Alter G, Broge T, Linde C, Ackerman ME, Brown EP, Borducchi EN, Smith KM, Nkolola JP, Liu J, Shields J, Parenteau L, Whitney JB, Abbink P, Ng’anga DM, Seaman MS, Lavine CL, Perry JR, Li W, Colantonio AD, Lewis MG, Chen B, Wenschuh H, Reimer U, Piatak M, Lifson JD, Handley SA, Virgin HW, Koutsoukos M, Lorin C, Voss G, Weijtens M, Pau MG, Schuitemaker H, Ng’anga DM, Seaman MS, Lavine CL, Perry JR, Li W, Colantonio AD, Lewis MG, Chen B, Wenschuh H, Reimer U, Piatak M, Lifson JD, Handley SA, Virgin HW, Koutsoukos M, Lorin C, Voss G, Weijtens M, Pau MG, Schuitemaker H. 2015. Protective efficacy of adenovirus-protein vaccines against SIV challenges in rhesus monkeys. *Science* 349:320–324. <https://doi.org/10.1126/science.aab3886>.
- Macpherson AJ, Harris NL. 2004. Interactions between commensal intestinal bacteria and the immune system. *Nat Rev Immunol* 4:478–485. <https://doi.org/10.1038/nri1373>.
- Macpherson AJ, Martinic MM, Harris N. 2002. The functions of mucosal T cells in containing the indigenous commensal flora of the intestine. *Cell Mol Life Sci* 59:2088–2096. <https://doi.org/10.1007/s00180200009>.
- Wu HJ, Wu E. 2012. The role of gut microbiota in immune homeostasis and autoimmunity. *Gut Microbes* 3:4–14. <https://doi.org/10.4161/gmic.19320>.
- Hooper LV, Macpherson AJ. 2010. Immune adaptations that maintain homeostasis with the intestinal microbiota. *Nat Rev Immunol* 10:159–169. <https://doi.org/10.1038/nri2710>.
- Wesemann DR, Portuguese AJ, Meyers RM, Gallagher MP, Cluff-Jones K, Magee JM, Panchakshari RA, Rodig SJ, Kepler TB, Alt FW. 2013. Microbial colonization influences early B-lineage development in the gut lamina propria. *Nature* 501:112–115. <https://doi.org/10.1038/nature12496>.
- Geuking MB, Cahenzli J, Lawson MAE, Ng DCK, Slack E, Hapfelmeier S, McCoy KD, Macpherson AJ. 2011. Intestinal bacterial colonization induces mutualistic regulatory T cell responses. *Immunity* 34:794–806. <https://doi.org/10.1016/j.immuni.2011.03.021>.
- Smith PM, Garrett WS. 2011. The gut microbiota and mucosal T cells. *Front Microbiol* 2:111. <https://doi.org/10.3389/fmicb.2011.00111>.
- Vossenkämper A, Blair PA, Safinia N, Fraser LD, Das L, Sanders TJ, Stagg AJ, Sanderson JD, Taylor K, Chang F, Choong LM, D’Cruz DP, MacDonald TT, Lombardi G, Spencer J. 2013. A role for gut-associated lymphoid tissue in shaping the human B cell repertoire. *J Exp Med* 210:1665–1674. <https://doi.org/10.1084/jem.20122465>.

20. Mouquet H, Nussenzweig MC. 2012. Polyreactive antibodies in adaptive immune responses to viruses. *Cell Mol Life Sci* 69:1435–1445. <https://doi.org/10.1007/s00018-011-0872-6>.
21. Haynes BF. 2005. Cardioliipin polyspecific autoreactivity in two broadly neutralizing HIV-1 antibodies. *Science* 308:1906–1908. <https://doi.org/10.1126/science.1111781>.
22. Goo L, Chohan V, Nduati R, Overbaugh J. 2014. Early development of broadly neutralizing antibodies in HIV-1-infected infants. *Nat Med* 20: 655–658. <https://doi.org/10.1038/nm.3565>.
23. Simonich CA, Williams KL, Verkerke HP, Williams JA, Nduati R, Lee KK, Overbaugh J. 2016. HIV-1 neutralizing antibodies with limited hypermutation from an infant. *Cell* 166:77–87. <https://doi.org/10.1016/j.cell.2016.05.055>.
24. Jost T, Lacroix C, Braegger CP, Chassard C. 2012. New insights in gut microbiota establishment in healthy breast fed neonates. *PLoS One* 7:e44595. <https://doi.org/10.1371/journal.pone.0044595>.
25. Pantoja-Feliciano IG, Clemente JC, Costello EK, Perez ME, Blaser MJ, Knight R, Dominguez-Bello MG. 2013. Biphasic assembly of the murine intestinal microbiota during early development. *ISME J* 7:1112–1115. <https://doi.org/10.1038/ismej.2013.15>.
26. Songjinda P, Nakayama J, Kuroki Y, Tanaka S, Fukuda S, Kiyohara C, Yamamoto T, Izuchi K, Shirakawa T, Sonomoto K. 2005. Molecular monitoring of the developmental bacterial community in the gastrointestinal tract of Japanese infants. *Biosci Biotechnol Biochem* 69:638–641. <https://doi.org/10.1271/bbb.69.638>.
27. Palmer C, Bik EM, DiGiulio DB, Relman DA, Brown PO. 2007. Development of the human infant intestinal microbiota. *PLoS Biol* 5:1556–1573. <https://doi.org/10.1371/journal.pbio.0050177>.
28. Lewis ZT, Totten SM, Smilowitz JT, Popovic M, Parker E, Lemay DG, Van Tassel ML, Miller MJ, Jin Y-S, German JB, Lebrilla CB, Mills DA. 2015. Maternal fucosyltransferase 2 status affects the gut bifidobacterial communities of breastfed infants. *Microbiome* 3:13. <https://doi.org/10.1186/s40168-015-0071-z>.
29. Kuang Y-S, Li S-H, Guo Y, Lu J-H, He J-R, Luo B-J, Jiang F-J, Shen H, Papasian CJ, Pang H, Xia H-M, Deng H-W, Qiu X. 2016. Composition of gut microbiota in infants in China and global comparison. *Sci Rep* 6:36666. <https://doi.org/10.1038/srep36666>.
30. Adlerberth I, Wold AE. 2009. Establishment of the gut microbiota in Western infants. *Acta Paediatr Int J Paediatr* 98:229–238. <https://doi.org/10.1111/j.1651-2227.2008.01060.x>.
31. Lin A, Bik EM, Costello EK, Dethlefsen L, Haque R, Relman DA, Singh U. 2013. Distinct distal gut microbiome diversity and composition in healthy children from Bangladesh and the United States. *PLoS One* 8:e53838. <https://doi.org/10.1371/journal.pone.0053838>.
32. Murphy K, Curley D, O'Callaghan TF, O'Shea C-A, Dempsey EM, O'Toole PW, Ross RP, Ryan CA, Stanton C. 2017. The composition of human milk and infant faecal microbiota over the first three months of life: a pilot study. *Sci Rep* 7:40597. <https://doi.org/10.1038/srep40597>.
33. Gomez-Arango LF, Barrett HL, McIntyre HD, Callaway LK, Morrison M, Nitert MD. 2017. Contributions of the maternal oral and gut microbiome to placental microbial colonization in overweight and obese pregnant women. *Sci Rep* 7:2860. <https://doi.org/10.1038/s41598-017-03066-4>.
34. McKenna P, Hoffmann C, Minkah N, Aye PP, Lackner A, Liu Z, Lozupone CA, Hamady M, Knight R, Bushman FD. 2008. The macaque gut microbiome in health, lentiviral infection, and chronic enterocolitis. *PLoS Pathog* 4:e20. <https://doi.org/10.1371/journal.ppat.0040020>.
35. Lozupone C, Stombaugh J, Gordon J, Jansson J, Knight R. 2012. Diversity, stability and resilience of the human gut microbiota. *Nature* 489: 220–230. <https://doi.org/10.1038/nature11550>.
36. Rodriguez JM, Murphy K, Stanton C, Ross RP, Kober OJ, Juge N, Avershina E, Rudi K, Narbad A, Jenmalm MC, Marchesi JR, Collado MC. 2015. The composition of the gut microbiota throughout life, with an emphasis on early life. *Microb Ecol Heal Dis* 26:26050. <https://doi.org/10.3402/mehd.v26.26050>.
37. National Research Council. 2011. Guide for the care and use of laboratory animals, 8th ed. National Academies Press, Washington, DC.
38. Narayan NR, Méndez-Lagares G, Ardeshir A, Lu D, van Rompay KKA, Hartigan-O'Connor DJ. 2015. Persistent effects of early infant diet and associated microbiota on the juvenile immune system. *Gut Microbes* 6:284–289. <https://doi.org/10.1080/19490976.2015.1067743>.
39. Ardeshir A, Narayan NR, Mendez-Lagares G, Lu D, Rauch M, Huang Y, Van Rompay KKA, Lynch SV, Hartigan-O'Connor DJ. 2014. Breast-fed and bottle-fed infant rhesus macaques develop distinct gut microbiotas and immune systems. *Sci Transl Med* 6:252ra120. <https://doi.org/10.1126/scitranslmed.3008791>.
40. Wiehe K, Easterhoff D, Luo K, Nicely NI, Bradley T, Jaeger FH, Dennison SM, Zhang R, Lloyd KE, Stolarchuk C, Parks R, Sutherland LL, Searce RM, Morris L, Kaewkungwal J, Nitayaphan S, Pitisuttithum P, Rerks-ngarm S, Sinangil F, Phogat S, Michael NL, Kim JH, Kelseo G, Montefiori DC, Tomaras GD, Bonsignori M, Santra S, Kepler TB, Alam SM, Moody MA, Liao H, Haynes BF. 2014. Antibody light-chain-restricted recognition of the site of immune pressure in the RV144 HIV-1 vaccine trial is phylogenetically conserved. *Immunity* 41:909–918. <https://doi.org/10.1016/j.immuni.2014.11.014>.
41. Liao H-X, Sutherland LL, Xia S-M, Brock ME, Searce RM, Vanleeuwen S, Alam SM, McAdams M, Weaver EA, Camacho ZT, Ma B-J, Li Y, Decker JM, Nabel GJ, Montefiori DC, Hahn BH, Korber BT, Gao F, Haynes BF. 2006. A group M consensus envelope glycoprotein induces antibodies that neutralize subsets of subtype B and CHIV-1 primary viruses. *Virology* 353: 268–282. <https://doi.org/10.1016/j.virol.2006.04.043>.
42. Liao H-X, Levesque MC, Nagel A, Dixon A, Zhang R, Walter E, Parks R, Whitesides J, Marshall DJ, Hwang K-K, Yang Y, Chen X, Gao F, Munshaw S, Kepler TB, Denny T, Moody MA, Haynes BF. 2009. High-throughput isolation of immunoglobulin genes from single human B cells and expression as monoclonal antibodies. *J Virol Methods* 158:171–179. <https://doi.org/10.1016/j.jviromet.2009.02.014>.
43. Kepler TB, Munshaw S, Wiehe K, Zhang R, Yu J-S, Woods CW, Denny TN, Tomaras GD, Alam SM, Moody MA, Kelseo G, Liao H-X, Haynes BF. 2014. Reconstructing a B-cell clonal lineage. II. Mutation, selection, and affinity maturation. *Front Immunol* 5:170. <https://doi.org/10.3389/fimmu.2014.00170>.
44. Kepler TB. 2013. Reconstructing a B-cell clonal lineage. I. Statistical inference of unobserved ancestors. *F1000Res* 2:103. <https://doi.org/10.12688/f1000research.2-103.v1>.
45. Sarzotti-Kelseo M, Bailer RT, Turk E, Lin CL, Bilska M, Greene KM, Gao H, Todd CA, Ozaki DA, Seaman MS, Mascola JR, Montefiori DC. 2014. Optimization and validation of the TZM-bl assay for standardized assessments of neutralizing antibodies against HIV-1. *J Immunol Methods* 409:131–146. <https://doi.org/10.1016/j.jim.2013.11.022>.
46. Montefiori DC, Karnasuta C, Huang Y, Ahmed H, Gilbert P, de Souza MS, McLinden R, Tovanabutra S, Laurence-Chenine A, Sanders-Buell E, Moody MA, Bonsignori M, Ochsenbauer C, Kappes J, Tang H, Greene K, Gao H, LaBranche CC, Andrews C, Polonis VR, Rerks-Ngarm S, Pitisuttithum P, Nitayaphan S, Kaewkungwal J, Self SG, Berman PW, Francis D, Sinangil F, Lee C, Tartaglia J, Robb ML, Haynes BF, Michael NL, Kim JH. 2012. Magnitude and breadth of the neutralizing antibody response in the RV144 and Vax003 HIV-1 Vaccine Efficacy Trials. *J Infect Dis* 206: 431–441. <https://doi.org/10.1093/infdis/jis367>.
47. Gray ES, Madiga MC, Moore PL, Misana K, Karim SSA, Binley JM, Shaw GM, Mascola JR, Morris L. 2009. Broad neutralization of human immunodeficiency virus type 1 mediated by plasma antibodies against the gp41 membrane proximal external region. *J Virol* 83:11265–11274. <https://doi.org/10.1128/JVI.01359-09>.
48. Saunders KO, Nicely NI, Wiehe K, Bonsignori M, Meyerhoff RR, Parks R, Walkowicz WE, Aussetat B, Wu NR, Cai F, Vohra Y, Park PK, Eaton A, Go EP, Sutherland LL, Searce RM, Barouch DH, Zhang R, Von Holle T, Overman RG, Anasti K, Sanders RW, Moody MA, Kepler TB, Korber B, Desaire H, Santra S, Letvin NL, Nabel GJ, Montefiori DC, Tomaras GD, Liao H-X, Alam SM, Danishefsky SJ, Haynes BF. 2017. Vaccine elicitation of high mannose-dependent neutralizing antibodies against the V3-glycan broadly neutralizing epitope in nonhuman primates. *Cell Rep* 18:2175–2188. <https://doi.org/10.1016/j.celrep.2017.02.003>.
49. Moody MA, Yates NL, Amos JD, Drinker MS, Eudailey JA, Gurley TC, Marshall DJ, Whitesides JF, Chen X, Foulger A, Yu J-S, Zhang R, Meyerhoff RR, Parks R, Scull JC, Wang L, Vandergrift NA, Pickeral J, Pollara J, Kelseo G, Alam SM, Ferrari G, Montefiori DC, Voss G, Liao H-X, Tomaras GD, Haynes BF. 2012. HIV-1 gp120 vaccine induces affinity maturation in both new and persistent antibody clonal lineages. *J Virol* 86:7496–7507. <https://doi.org/10.1128/JVI.00426-12>.
50. Younge N, Yang Q, Seed PC. 2017. Enteral high fat-polyunsaturated fatty acid blend alters the pathogen composition of the intestinal microbiome in premature infants with an enterostomy. *J Pediatr* 181:93–101. <https://doi.org/10.1016/j.jpeds.2016.10.053>.
51. Gu C. 2014. Smoothing spline ANOVA models: R package gss. *J Stat Softw* 58:1–25. <https://doi.org/10.18637/jss.v058.i05>.